Geophysical Journal International

Geophys. J. Int. (2014) **199,** 707–716 doi: 10.1093/gji/ggu247

GJI Geomagnetism, rock magnetism and palaeomagnetism

High-temperature susceptibility of magnetite: a new pseudo-single-domain effect

David J. Dunlop

Department of Physics, University of Toronto, Toronto, ON M5S 1A7, Canada. E-mail: dunlop@physics.utoronto.ca

Accepted 2014 June 26. Received 2014 June 25; in original form 2014 April 15

SUMMARY

Remanent magnetizations of magnetites between single-domain (SD) threshold size (≈0.1 μm) and ≈20 μm have SD-like intensities and coercivities. This paper shows for the first time that magnetite's induced magnetization also has pseudo-single-domain behaviour. The first part of the paper reports temperature-dependent initial susceptibility data, $k_0(T)$, of sized magnetites and assesses their granulometric potential. The second part transforms coercive force data, $H_c(T)$, for the same magnetites into simulated $k_0(T)$ curves. The third part considers $k_0(T)$ results of coarse-grained mafic rocks as candidate sources of deep-seated magnetic anomalies.

High-temperature susceptibility k_0 measured with a Kappabridge for eight fractions of crushed natural magnetites (median sizes of 0.6, 1, 3, 6, 9, 14, 110 and 135 μm) shows a progressive increase in the height of the Hopkinson peak below the Curie point as grain size decreases. The trend is systematic and has granulometric potential in the 1–14 μm range. Self-demagnetization should produce almost flat $k_0(T)$ in grains larger than SD size but experimentally, well-defined Hopkinson peaks are not limited to the finest grains. 1-μm magnetites have a peak 1.5 times k_0 at 20 °C and 14-μm grains have a peak of 1.25. Only 110 and 135 μm grains have T-independent k_0.

Using an empirical relationship between coercive force H_c and k_0, $H_c(T)$ data for the sized magnetites were used to simulate $k_0(T)$ results. A hump in the k_0 heating curve around 250 °C was traced to annealing out internal strains, evident in H_c data measured in first heatings. For sizes ≤6 μm, observed Hopkinson peaks were smaller than predicted, possibly because of a previously unrecognized grain-size dependence of the empirical constant relating H_c and k_0.

Two crystalline rocks, a gabbro and a diabase, combine SD-like Hopkinson peaks and multidomain (MD) flat ramps in their $k_0(T)$ data. In the diabase, a Hopkinson peak is prominent in separated plagioclase grains containing submicron magnetite, but is masked in whole-rock data. The gabbro has a clear superposition of SD and MD $k_0(T)$ functions in its whole-rock data, with a Hopkinson peak of 1.35. If oceanic layer-3 gabbros have similar susceptibility enhancement above 500 °C, they could be more important magnetic anomaly sources than room-temperature k_0 measurements on dredged or fault-uplifted samples would suggest.

Key words: Magnetic anomalies: modelling and interpretation; Magnetic and electrical properties; Magnetic mineralogy and petrology; Rock and mineral magnetism.

1 INTRODUCTION

Ferromagnetic substances undergo a profound change in structure at the single-domain (SD) threshold size d_0. Above this size, they are no longer uniformly magnetized in their zero-field (remanent) state but develop a spin vortex (Harrison *et al.* 2002), which in still larger grains nucleates a domain wall separating two oppositely magnetized domains. In magnetite (Fe_3O_4), the expected abrupt change from near-saturation magnetic moment in the SD state to almost zero moment in slightly larger vortex or two-domain grains is not seen in macroscopic magnetic properties. Thermoremanent magnetization (TRM) and other remanences change continuously with increasing grain size, bridging from d_0 (≈0.1 μm in magnetite) to 10–20 μm. The coercivity—the resistance of these remanences to changes in magnetic field—also drops off gradually, not discontinuously, in larger grains.

Although the mechanism remains poorly understood, this pseudo-single-domain (PSD) phenomenon is vitally important in palaeomagnetism (Dunlop 2012). Only a minute fraction of the magnetite in most rocks is small enough to be SD. PSD magnetite covers a much broader size range and records palaeomagnetic signals of almost SD strength which can endure for millions of years, in contrast

to the weak and changeable remanence of multidomain (MD) grains containing numerous domains and mobile walls.

PSD behaviour has been assumed to be a property of remanent magnetization, originating in the failure of grains to nucleate walls (Halgedahl & Fuller 1983) or in nuclei or sections of domains which are pinned by defects in the crystal lattice. The work described in this paper shows that this view is too narrow. The initial weak-field AC susceptibility of magnetite in 1–15 μm sizes also exhibits PSD behaviour. This reversible dynamic response to small field changes cannot be due to nucleation failure nor to jumps of walls bounding domains or domain nuclei. Nucleation and wall jumps are irreversible processes and unlikely to occur in the weak fields used to measure initial susceptibility.

Induced magnetization $\boldsymbol{M}$ in field $\boldsymbol{H}$, starting initially from $\boldsymbol{M} = 0$, obeys Rayleigh's law:

$$M = k_0 H + BH^2. \quad (1)$$

In (1) k_0 is the initial reversible susceptibility and the second Rayleigh coefficient B is related to irreversible processes (nucleation, wall jumps). The initial susceptibility k is the limit of M/H:

$$k = k_0 + BH \rightarrow k_0 \text{ as } H \rightarrow 0. \quad (2)$$

The dependence of k_0 on temperature T is important as a laboratory method of identifying magnetic minerals by their phase transitions and in interpreting magnetic anomalies because k_0 tends to increase at high T, for example, in the deep crust or uppermost mantle. Both applications make use of the Hopkinson effect (Hopkinson 1889; Dunlop & Özdemir 2007, pp. 311–313), a peak in k_0 which occurs just below the Curie temperature T_C or flanks other phase transitions like the low-temperature Verwey transition in magnetite. The underlying cause of the Hopkinson peak is the unpinning of domain walls in MD grains or of grain magnetic moments in SD grains, both of which increase magnetization in the direction of the ambient field $\boldsymbol{H}$. The coercive force H_c measured in hysteresis loops decreases with SD or MD unpinning. With increasing T, H_c therefore drops while k_0 rises. These changes in H_c and k_0 may be accompanied by irreversible remanence unblocking: in SD grains, a large Hopkinson peak is associated with concentrations of high unblocking temperatures (Dunlop 1974).

However, the situation is complicated in MD grains by self-demagnetization, which restrains any tendency to increase net magnetization. The internal self-demagnetizing field exists also in SD grains but is ineffectual because SD moments are created by strong exchange coupling of spins and are for all practical purposes permanent: only their orientations can be altered, not their magnitudes. In MD grains, on the other hand, domains magnetized in or near the direction of $\boldsymbol{H}$ enlarge while unfavourably oriented domains shrink, so that the net moment can potentially increase enormously as pinning of the walls between domains weakens. However, any increase in net magnetization $\boldsymbol{M}$ creates an opposing demagnetizing field $\boldsymbol{H}_d = -N\boldsymbol{M}$ which counteracts the effect of the external field $\boldsymbol{H}$. The demagnetizing factor N is determined by the grain's shape and domain geometry (Dunlop & Özdemir 1997, chapters 4 and 5).

The intrinsic ('true') susceptibility $k_i = \mathrm{d}M/\mathrm{d}H_i$, describing the response of $\boldsymbol{M}$ to the total internal field $\boldsymbol{H}_i = \boldsymbol{H} + \boldsymbol{H}_d = \boldsymbol{H} - N\boldsymbol{M}$, is not directly measurable. External measurements on the sample yield only the observed susceptibility $k_0 = \mathrm{d}M/\mathrm{d}H$. The two susceptibilities are related by

$$k_0(T) = k_i(T)[1 + Nk_i(T)]^{-1} \rightarrow N^{-1} \text{ if } k_i \gg k_0. \quad (3)$$

The braking effect of $\boldsymbol{H}_d$ can cause k_0 to be very much less than k_i in MD grains of highly susceptible materials like iron (studied by Hopkinson) or magnetite. The Hopkinson peak in $k_0(T)$ that characterizes SD grains near a critical point like T_C is muted at best in MD grains. If $k_i \gg k_0$, as is typically the case for coarse-grained magnetite, k_0 approaches the temperature independent value $1/N$ and $k_0(T)$ is a flat ramp which drops abruptly to zero at T_C without any noticeable peak.

There is an indirect way of making $k_i(T)$ visible. Empirically for 1.5–80-μm magnetite

$$k_i H_c \approx 45 \text{ kA m}^{-1}, \quad (4)$$

(Stacey & Banerjee 1974, p. 74). Unlike susceptibilities, H_c is unaffected by self-demagnetization. This comes about because H_c is the axis-crossing point in a hysteresis loop, measured when $M = 0$ and $\boldsymbol{H}_i = \boldsymbol{H}$. We can therefore generate simulated values of k_i using its inverse relationship with H_c. The theory leading to (4) refers to room-temperature domain structures and H_c data. The assumption that the constant on the r.h.s. of (4) has the same value at higher temperatures will be tested later.

This paper has three main purposes. The first is to report $k_0(T)$ data (heating and cooling curves) for a set of sized magnetites and to assess their granulometric potential. The second is to transform measured $H_c(T)$ data for the same samples into $k_i(T)$ curves using (4) and thence into simulated $k_0(T)$ curves using (3), for comparison with the measured $k_0(T)$ results. The final purpose is to analyse $k_0(T)$ results of some coarse-grained mafic rocks showing a superposition of SD-like Hopkinson peaks and MD-type flat ramps and to consider their possible role as a source of deep-seated magnetic anomalies.

2 EXPERIMENTAL METHODS AND SAMPLE CHARACTERIZATION

Initial susceptibility k_0 was measured with a Geofyzika KLY-2 Kappabridge variable-temperature AC susceptibility bridge, which uses a 920 Hz alternating field ($H = 0.3$ kA m^{-1} rms). Measurements of k_0 were recorded every ≈3 °C during heating from $T = 20$ °C to 650–700 °C and cooling back to ≈50 °C. Flowing Ar gas was used to inhibit oxidation of the finest magnetite powders (0.6, 1 and 3 μm) at high T. A complete heating-cooling run took about 2 hr.

Coercive force H_c was determined from hysteresis (M versus H) loops measured every 20 °C from room temperature to 600 °C. Other parameters determined routinely were saturation remanence M_{rs} and saturation magnetization M_s. The usual maximum field used was 0.5 T (≈400 kA m^{-1}). The *M-H-T* measurement sequence was pre-programmed on a Princeton Measurements micro-VSM (vibrating-sample magnetometer). Oxidation at high temperatures was inhibited by flowing He gas. A complete set of hysteresis measurements required about 6 hr, including a repeat run at 20 °C after cooling from peak temperature.

Susceptibility and some hysteresis results are reported for two Precambrian rocks, the Matachewan Diabase (northwestern Ontario, Canada) and the Michael Gabbro (Labrador, Canada). The main reason for including them in this study was their bimodal distribution of magnetite grain sizes. The magnetite occurs both as discrete coarse grains in the silicate matrix and as fine inclusions precipitated from and enclosed within particular silicate minerals, principally plagioclase and actinolite. The coarse grains are magnetically MD, containing many domains and walls. The finest magnetite inclusions approach SD size (Dunlop *et al.* 2005).

Because of the sometimes complicated mineralogical changes that can alter the magnetic behaviour of rocks during laboratory heating, even in controlled atmospheres, the main set of

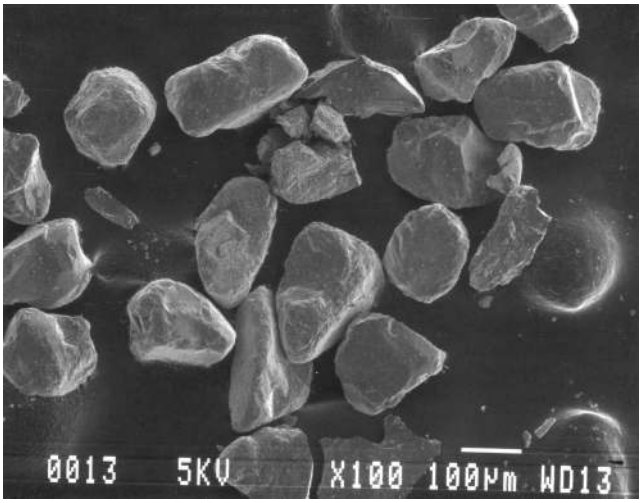

Figure 1. Scanning electron micrograph of the coarsest grain-size fraction of crushed magnetite after a first sieving (125–150 μm mesh). Grains are subhedral with a median particle dimension of 135 μm, with some adhering finer fragments.

susceptibility and hysteresis experiments was carried out on sized fractions of pure magnetite. Large natural single crystals from Bancroft, Ontario, Canada were crushed by mortar and pestle. Coarse size fractions were obtained by sieving and seven fine fractions were separated from the residue using a Bahco centrifugal dust analyser. Fig. 1 is a scanning electron micrograph after a first sieving of the coarsest fraction. The grains are more or less equidimensional with sizes in the 125–150 μm range (median size: 135 μm). A few smaller fragments can be seen; these are more angular and irregular in shape. They were separated as much as possible by agitation and re-sieving, adding to the residue for centrifuging. Data for two coarse fractions (mean particle dimensions of 110 and 135 μm) and six fine fractions (0.6, 1, 3, 6, 9 and 14 μm) are reported here. In the case of the 9-μm magnetite, only the k_0 cooling curve was usable. Another fraction (20 μm mean size) unfortunately gave no usable $k_0(T)$ results because of malfunction of the bridge.

3 SUSCEPTIBILITY RESULTS FOR THE ROCK SAMPLES

Susceptibility versus temperature results for a plagioclase separate from Matachewan Diabase sample TK49 are noisy but rise to a pronounced peak in k_0 at about 560 °C (heating curve), just below the magnetite Curie point, $T_C = 585$ °C (Fig. 2a). The Hopkinson peak, $(k_0)_{max}/(k_0)_{20} \approx 4$, in Fig. 2(a) is quite large, larger in fact than the Hopkinson peak reported by Dunlop (1974) for elongated SD grains of magnetite. There is a sizeable peak in the cooling curve as well but shifted to slightly lower temperature. The vertical offset of the two curves is a machine artifact.

Since SD moments cannot change their magnitudes appreciably in response to $\boldsymbol{H}$, what is the source of these large Hopkinson peaks? The induced magnetization of SD grains is small at room temperature because the moment of each grain is tightly bound to one or more easy axes by shape or crystalline anisotropy. It can only make small reversible rotations away from the easy axis in response to small applied fields. As T rises, anisotropy forces weaken and the rotations increase in size, producing a somewhat larger k_0. However, the major change occurs at the grain's blocking temperature T_B, where pinning by anisotropy is overcome by thermal agitation. In this thermal equilibrium state of superparamagnetism, k_0 increases enormously, in accord with a Langevin law analogous to that for paramagnetism but with giant ('super') moments. The superparamagnetic Hopkinson peak height is limited mainly by the eventual drop in spontaneous magnetization M_s to zero at T_C.

In large MD grains with many domains, reversible displacements of unpinned sections of domain boundaries play the same role in induced magnetization as small-angle moment rotations in SD grains. However, a new factor comes into play. Self-demagnetization opposes any increase in net magnetization and limits k_0 to a value $\leq 1/N$, as explained earlier. MD k_0 is thus nearly independent of temperature, exhibiting at most a minor peak very close to T_C (Clark & Schmidt 1982). The whole-rock results for TK49 exhibit MD behaviour (Fig. 2b).

The heating curve of the Michael Gabbro illustrates T-independent to gently increasing MD k_0 (up to ≈400 °C) and an SD peak in k_0 at the highest temperatures (Fig. 2c). This superposition of two k_0(T) behaviour patterns must be due to the bimodal nature of the rock. Coarse-grained groundmass magnetite dominates k_0 until superparamagnetically enhanced k_0 of the plagioclase inclusions grows large enough to show through as an SD Hopkinson peak. [In the case of TK49, the plagioclase fraction was too small to show through in whole-rock measurements (Fig. 2b).] The Michael Gabbro cooling curve is interesting. If renormalized to the ultimate room-temperature value of k_0 after cooling, the Hopkinson peak $(k_0)_{max}/(k_0)_{20} = 1.4$, similar to $(k_0)_{max}/(k_0)_{20} = 1.35$ for the heating curve. However, in detail the cooling curve is more complex. After retracing the original curve up to its peak, the cooling curve continues to climb, revealing a new magnetic phase with a lower T_C whose Hopkinson peak is sharper than the heating peak but tails off more gradually in cooling.

4 SUSCEPTIBILITY RESULTS FOR THE SIZED MAGNETITES

Judging by the flat k_0 versus T heating curve, lacking any Hopkinson peak (Fig. 3a), domains in the 110-μm magnetite grains respond readily to self-demagnetizing fields. The 135-μm magnetite sample gives similar results (illustrated later). This comes as no surprise because well-developed domains bounded by mobile 71°, 109° and 180° walls are observed in magnetite crystals of about this size (Özdemir *et al.* 1995).

Susceptibility peaks in the heating curves of the centrifuged magnetite samples rise above the plateau of the 110 μm $k_0(T)$ data in Fig. 3(a), increasing progressively from $(k_0)_{max}/(k_0)_{20} = 1.27$ for the 14 μm grains to 1.52 for the 1-μm grains. The 0.6 μm size fraction has a much higher peak but its diagnostic value is actually inferior to that of the lower peaks of the 1–14-μm magnetites. This is because the 0.6 μm fraction is the final residue after centrifuging and has a much broader size spread than the other fractions. It may possibly contain enough truly SD material to bias the peak height through superparamagnetic enhancement.

Susceptibility peaks in the cooling curves (Fig. 3b) mirror the pattern seen in the heating curves over the same grain size range. One difference is that the subsidiary peaks or inflections around 250 °C in the heating curves are muted or absent in the cooling curves. These minor peaks are related to lattice strains introduced in crushing the starting material. The strains are partially (although not completely) annealed out in the first heating to 650–700 °C. Independent evidence for this interpretation comes from H_c versus T data measured in first and subsequent heatings (next section).

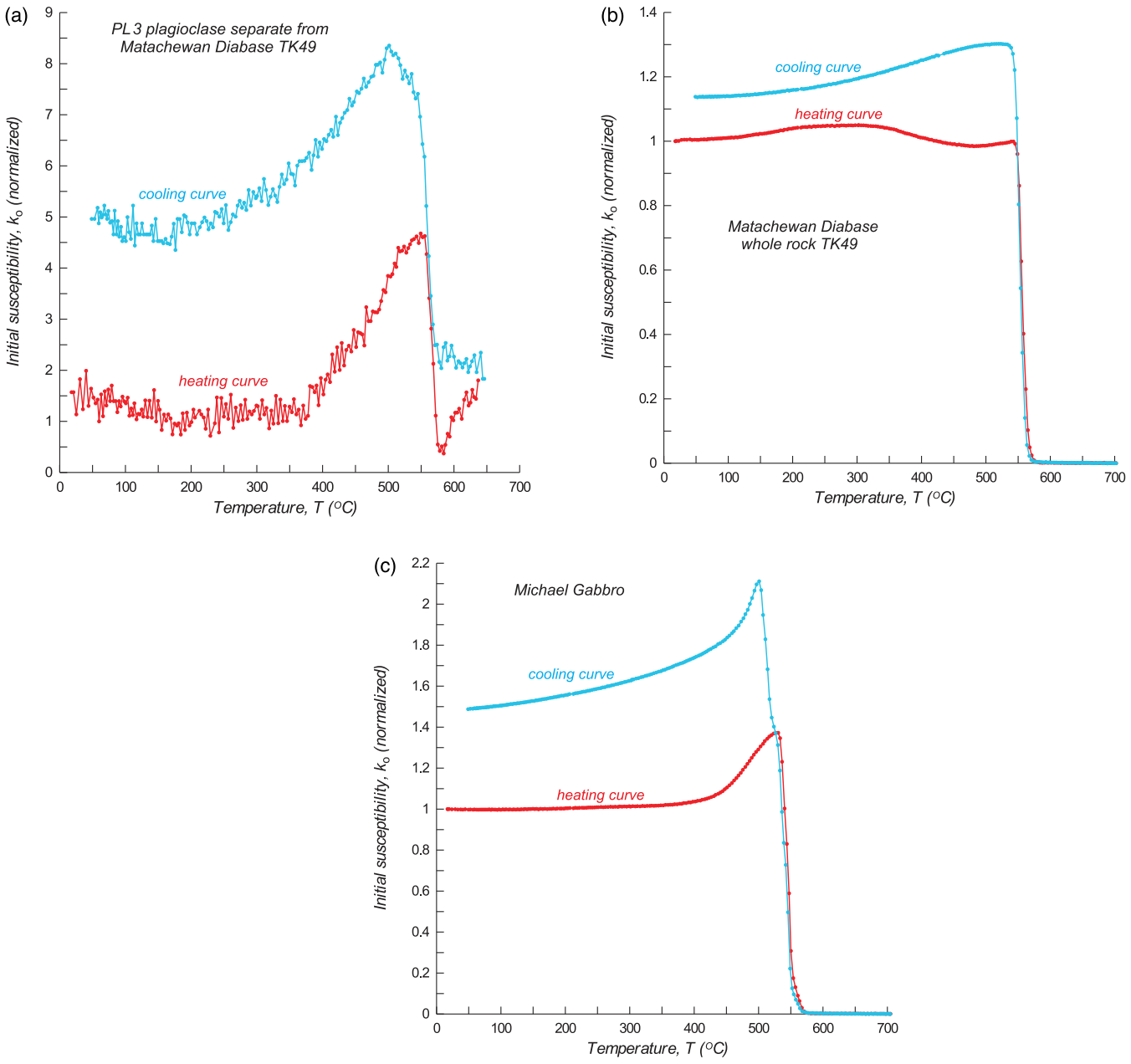

Figure 2. Kappabridge measurements of initial susceptibility k_0 as a function of temperature T for two rocks with bimodal magnetite grain-size distributions. (a) Plagioclase containing submicroscopic magnetite inclusions from sample TK49 of the ≈2.6 Ga Matachewan Diabase shows marked single-domain Hopkinson peaks on heating and cooling. (b) The plagioclase signal is masked in the TK49 whole-rock results, which are dominated by the multidomain response of coarse groundmass magnetite. (c) A whole-rock sample of the ≈1.4 Ga Michael Gabbro shows superimposed flat or ramp-like multidomain k_0–T behaviour (below 400 °C, heating curve) and sharp single-domain-type Hopkinson peaks (500–550 °C, heating and cooling curves).

5 HYSTERESIS RESULTS FOR THE SIZED MAGNETITES

Room-temperature hysteresis parameters M_{rs}/M_s and H_c of the sized magnetite samples are listed in Table 1. Most are for unannealed samples, the starting material for the temperature-dependent hysteresis measurements described below. In four cases (0.6, 3, 6 and 14 μm), comparison values are given for fully annealed samples. Two trends are evident. M_{rs}/M_s and H_c values decrease with increasing grain size in a regular and expected way (Dunlop & Özdemir 1997, figs 12.3, 12.4) and annealing reduces both coercivity and remanence.

Major-loop hysteresis parameters M_s, M_{rs} and H_c are plotted as a function of measurement temperature T for four representative samples in Figs 4(a)–(d). Values in the first and the second or third heatings are normalized to the initial M_s, M_{rs} or H_c values at the outset (20 °C) of run 1. All parameters decrease with increasing temperature but at different rates. $M_s(T)$ decreases slowly at first, then increasingly rapidly until it vanishes at the Curie point T_C, which is 575–585 °C according to these results. (Measurements at 20 °C intervals do not permit a very precise determination of T_C given the rapid descent of M_s. Unfortunately, it is difficult to override the program and substitute smaller T steps in a selected

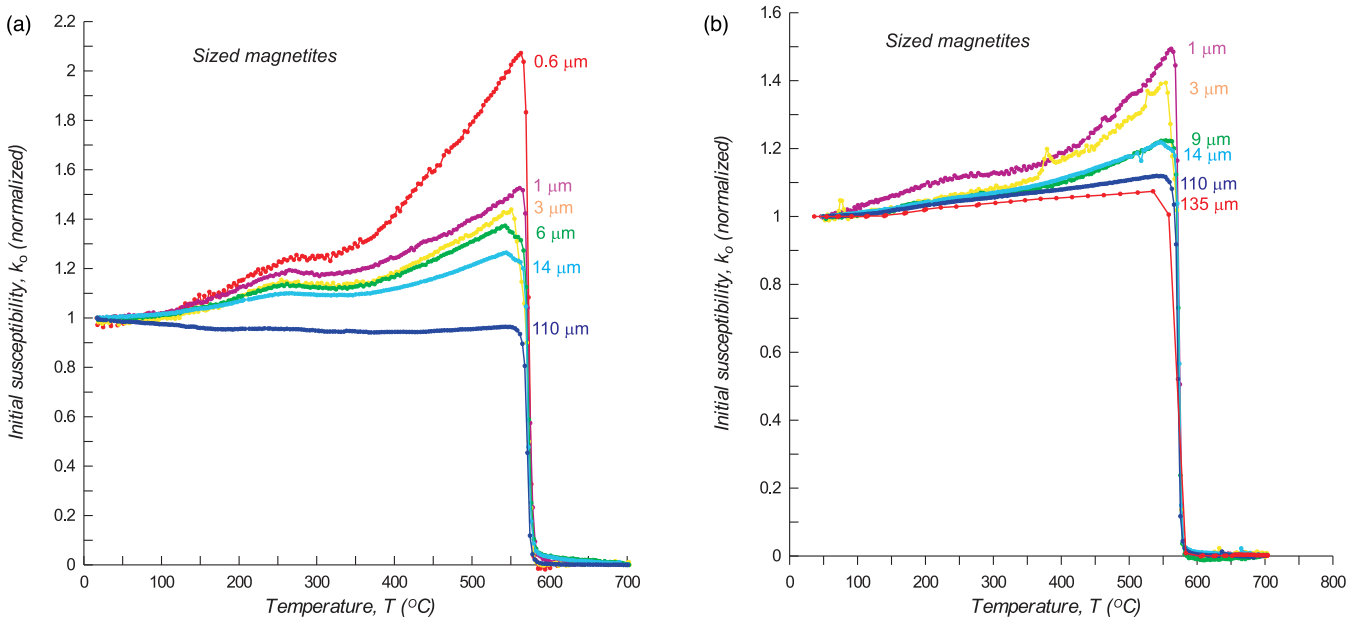

Figure 3. A selection of Kappabridge k_0–T curves measured in flowing Ar for various size fractions of crushed natural magnetites. All curves are normalized to k_0 values measured at 20 °C (a, heating curves, initial values) or at 50 °C (b, cooling curves, terminal values). There is a regular upward progression of Hopkinson peak heights as grain size decreases. The k_0–T curves evolve from multidomain flat ramps with no marked peak (110 and 135 μm) to sharp single-domain-like peaks for the 0.6, 1 and 3 μm magnetites (which are much larger than the critical single-domain size of ≈0.1 μm). Humps in the k_0–T curves around 250 °C (prominent in heating curves, more subdued in cooling curves) are due to lattice strains produced by crushing, which partially anneal out in the first heating to 700 °C (see Figs 4 and 6).

Table 1. Hysteresis parameters of the sized magnetite samples at 25 °C.

Mean grain size, d (μm)	Saturation remanence ratio, M_{rs}/M_s		Coercive force, $\mu_0 H_c$ (mT)	
0.6	0.316 (U)	0.207 (A)	32.1 (U)	17.8 (A)
1	0.222		21.0	
3	0.158	0.093	15.9	9.53
6	0.129	0.062	12.4	6.66
9	0.098		10.2	
14	0.080	0.040	7.58	4.03
20	0.047		6.44	
110	0.014		2.83	
135	0.009		1.35	

U, unannealed; A, annealed.

interval. Possible, but unknown, drift in temperature over the ≈10 min taken to measure a loop limits the ultimate resolution. There could also be a small T difference between the locations of the sample and the thermocouple.)

The shapes of the M_s(T) curves are reproducible from one run to the next (except for the 0.6-μm magnetite) and from sample to sample. This is as expected since M_s in 0.5 T approximates to the spontaneous magnetization of magnetite, which is sample invariant. The 20 °C value of M_s does not change after the first heating, even in the 0.6 μm fraction. Evidently the He flow was generally effective in inhibiting oxidation.

Although chemical alteration has not occurred to any great extent, microstructural alteration is evident in the M_{rs} and H_c data. Both the shapes and the absolute values of the $M_{rs}(T)$ and $H_c(T)$ curves are very different from one run to another. However, remarkably enough the shapes of the two curves are very similar in any particular run: $M_{rs}(T) \sim H_c(T)$. This is understandable for large MD magnetites because self-demagnetization theory predicts that the slope of the descending hysteresis curve between the M-axis and H-axis crossing points is the same as the slope of the initial magnetization curve (i.e. k_0), namely $1/N$. Thus, $M_{rs} \approx H_c/N$ (Dunlop & Özdemir 1997, eq. (5.32)). Yet the existence of substantial Hopkinson peaks in the 14 μm, 1 μm and especially the 0.6 μm samples is firmly opposed to the notion of strict magnetostatic control, which should result in featureless $k_0(T)$ ramps.

Returning to the evidence for microstructural alteration of the magnetites, Figs 4(a)–(c) show that H_c (and M_{rs} in step with it) decrease strongly above 100 °C, pass through a point of minimum slope around 250 °C and finally return to a normal descent above 300 °C. In second and third heating runs, the $M_{rs}(T)$ and $H_c(T)$ curves descend monotonically and reproducibly. In each case, M_{rs} and H_c values in the second (or third) run are substantially lower than the starting values for the unheated samples, but approach the run 1 M_{rs} or H_c curves above 300 °C. A decrease in the capacity for wall pinning has occurred during the first heating, and at comparatively low temperatures. The most straightforward explanation is that strains introduced into the lattice by crushing the original magnetite crystals have partially annealed out.

The same phenomenon is presumably at the root of the peaks/inflections in $k_0(T)$ curves around 250 °C (Figs 3a and b). The heating and cooling are more rapid in these experiments and annealing is less effective. The 250 °C peaks/inflections, although reduced, do not completely disappear from the cooling curve. Note the lack of peaks or inflections in $k_0(T)$, $M_{rs}(T)$ or $H_c(T)$ results for the TK49 plagioclase, whose magnetite is virginal (Figs 2a and 4d).

6 DISCUSSION

6.1 Granulometric potential of the 1–14 μm $k_0(T)$ data

The regular increase in Hopkinson peak heights with decreasing grain size can be judged from Fig. 5. Over the range $d = 1$ to 14 μm,

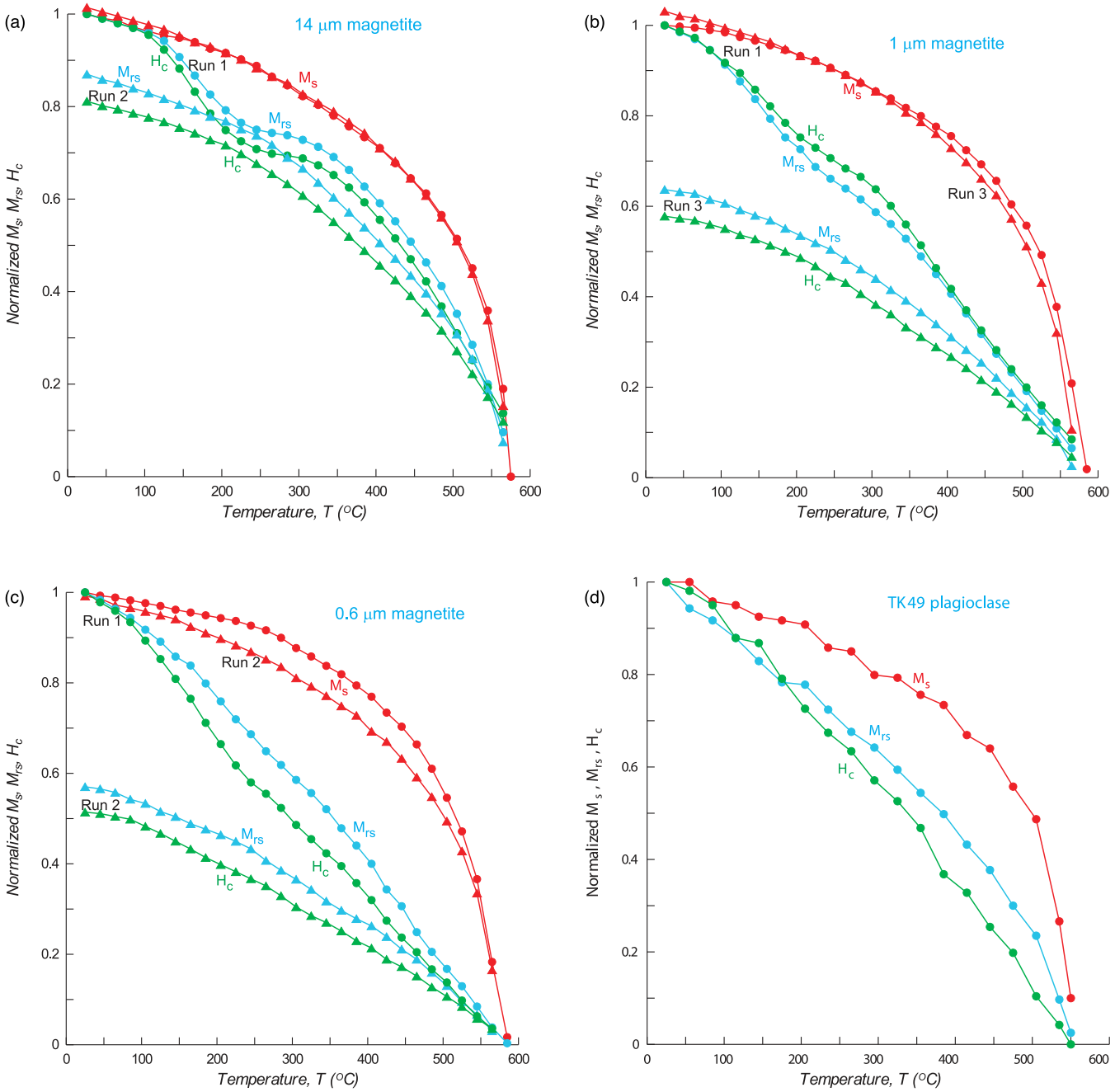

Figure 4. Hysteresis parameters M_s (saturation magnetization in 0.5 T), M_{rs} (saturation remanence) and H_c (coercive force) measured at 20 °C intervals with a micro-VSM (vibrating-sample magnetometer) for (a) 14 μm, (b) 1 μm, (c) 0.6 μm magnetites and (d) TK49 plagioclase containing submicroscopic magnetite. He gas flow inhibited oxidation at high temperatures. Values of each parameter in 2nd or 3rd heating runs are normalized to 20 °C initial values in run 1. $M_s(T)$ does not change much between the 1st and later runs but $M_{rs}(T)$ and $H_c(T)$—which track each other closely in all runs—have irreversible dips and recoveries in the 1st run which are absent from later runs. This phenomenon is interpreted as resulting from the annealing out of initial lattice strains in the 6 hr 1 st heatings. Both $M_{rs}(T)$ and $H_c(T)$ values are reduced as a result between the 1st and subsequent runs.

the mean of the $(k_0)_{max}/(k_0)_{20}$ values measured in heating and in cooling decreases linearly with log d from ≈1.5 to ≈1.25. Although data for grain sizes between ≈15 and ≈100 μm are lacking, it is interesting that the trends in Fig. 5 project to 1.0–1.1 in the range 100–150 μm. This is the range of $(k_0)_{max}/(k_0)_{20}$ observed in cooling curves for the 110 and 135 μm samples (Figs 3b and 6a).

King & Ranganai (2001) report a progression in Hopkinson peak heights for magnetites with average sizes in the 0.1–1 μm interval. However, their $(k_0)_{max}/(k_0)_{20}$ values are 1.13, 1.22, 1.42 and 1.7 for 1, 0.5, 0.2 and 0.1 μm, respectively. The 0.1 μm value of 1.7 falls on the projection of the trend in Fig. 5 but the other values decrease rapidly (and nonlinearly) as the grain size increases. Their 1 μm $(k_0)_{max}/(k_0)_{20}$ value of 1.13 is only slightly above our 110 μm peak height.

Many of King & Ranaganai's magnetites were produced as 2-D arrays of regularly spaced crystals by electron-beam lithography (King *et al.* 1996; King & Williams 2000). It may be that particle geometry and/or interparticle interaction are at the root of the

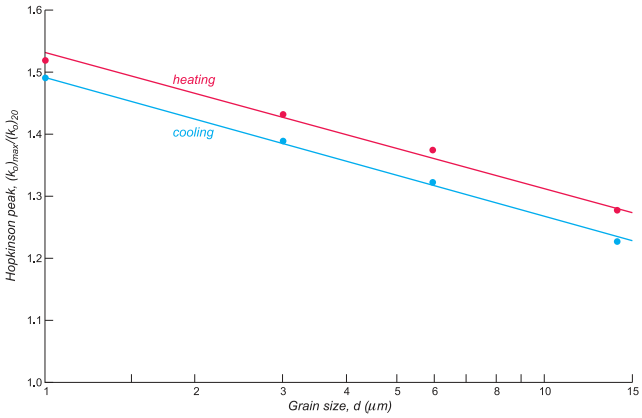

Figure 5. Hopkinson peak heights $(k_0)_{max}/(k_0)_{20}$ have pseudo-single-domain magnitudes of 1.25–1.5 over a size range 1–14 μm, which is 1–2 orders of magnitude larger than magnetite's critical SD size $d_0 \approx 0.1$ μm (and 2–7 orders of magnitude larger in volume than critical SD volume). The regular decrease of $(k_0)_{max}/(k_0)_{20}$ with log d, if projected to larger d, incorporates the 1–1.1 peak heights for the 110 and 135 μm magnetites (multidomain limit). If projected downward in d, towards d_0, it also incorporates the value 1.7 reported by King & Ranganai (2001) for 0.1 μm magnetite. However, their values of 1.42, 1.22 and 1.13 for 0.2, 0.5 and 1 μm magnetites are incompatible with the linear trends in Fig. 5, as is their 40 μm value of 1.02.

disagreement between the present results and theirs but clearly more work is needed before Hopkinson peaks become a standard tool for determining magnetite grain size. This is a pity because other widely used methods such as FORC diagrams (Roberts *et al.* 2000) and Day plots (Dunlop 2002a,b) respond to domain structure (SD, PSD, MD) and only determine grain size indirectly. The Hopkinson effect is also appealing because it indicates approximately the Curie temperature and thus directly flags any cation deficiencies or impurities in the magnetite.

6.2 Susceptibility enhancement in deep-seated rocks

There has been much discussion of the question of 'missing magnetization': the inadequacy of susceptibilities of rocks commonly sampled at Earth's surface in explaining major magnetic anomalies over continents and oceans, claimed by some and disputed by others (see Dunlop (2010) for a summary). One idea that has surfaced periodically is possible enhancement of the induced magnetic signal of rocks located at depths where the ambient temperature approaches the Curie point (e.g. Dunlop 1974; Arkani-Hamed 1989; Kiss *et al.* 2005, 2008; Szarka *et al.* 2007, 2010). The Curie-point isotherm near spreading ridges lies in the mid-crust for MORB titanomagnetites ($T_C \approx 150$–$250\,^\circ$C) and in the deep crust or upper mantle for magnetite in gabbros and serpentinites. Under continents, magnetite probably approaches 550 °C, with potentially enhanced k_0, at mid-crustal to Moho depths.

Data on the Hopkinson peak in rocks does exist in the literature (e.g. Kontny & de Wall 2000; Ferré *et al.* 2012a,b) but $k_0(T)$ measurements are most commonly made to determine a rough value for T_C and hence magnetic mineralogy. The shape of the curve and presence or absence of a peak is seldom mentioned. Williams *et al.* (1985) and Shive & Fountain (1988) published Hopkinson curves for uplifted deep continental rocks and concluded that flat MD ramps with insignificant thermal peaks were the norm. The whole-rock Matachewan Diabase results demonstrate that even when suitable fine-grained magnetite is present, its signal may be masked by that of coarser grains (Figs 2a and b). On the other hand, the Michael Gabbro data (Fig. 2c) show that enhancement factors of ≈40 per cent do exist. Similar enhancements were reported for Variscan gneisses sampled at depths of up to 3.5 km by Dubuisson *et al.* (1991) and for oceanic gabbros by Pozzi & Dubuisson (1992). The question remains open.

6.3 Synthesizing $k_0(T)$ using $H_c(T)$ data

The procedure for synthesizing $k_0(T)$ was outlined in Section 1. Using $k_i\ H_c \approx 45$ kA m^{-1} (eq. 4), $H_c(T)$ generates a set of $k_i(T)$ pseudo-data. These are transformed into $k_0(T)$ pseudo-data using $k_0(T) = k_i(T)\ [1 + N\ k_i(T)]^{-1}$ (eq. 3). Some representative results of the calculations appear in Fig. 6.

Both k_i and H_c are controlled by the shapes of energy barriers to wall motion or $E_w(x)$, where x represents wall displacement. In null field, each wall is located near a minimum in E_w. Small excursions about the minimum give rise to induced magnetization. The smaller the local dE_w/dx, the greater are the excursions and the larger is k_i (in terms of the local internal field), and taking self-demagnetization into account, also the value of k_0 observed outside the magnetite sample. Larger fields can drive walls beyond the point of steepest slope $(dE_w/dx)_{max}$ of a local energy well; the average of these fields is H_c. A constant value for the r.h.s. of eq. (4) of 45 kA m^{-1} for magnetites of different grain sizes would imply that energy wells in large and small grains have different amplitudes but the same basic shape, so that dE_w/dx near the minimum is a constant fraction of $(dE_w/dx)_{max}$. Since H_c and k_i are, respectively, proportional and inversely proportional to energy gradient, $k_i\ H_c$ would then have a constant value at any temperature, whence eq. (4).

Large grains contain more walls and these walls are more mobile than in small grains. The energy wells are shallower, so that H_c is smaller and k_i is larger. Even if the anisotropy that governs the shapes of energy barriers decreases at the same rate for small and large MD grains [i.e. $H_c(T)$ is the same for both], larger k_i values lead to stronger self-demagnetizing fields and k_0 should be less temperature dependent for the large grains. This is the source of the trend observed for most of the samples tested (but not for all as the next paragraph shows).

Best agreement between real $k_0(T)$ data and values predicted from $H_c(T)$ was for the larger grains: 14, 110 and 135 μm. Although self-demagnetization should affect all large MD grains in much the same way, $k_0(T)$ results (both measured and simulated) are different for the 110 and 135 μm magnetite size fractions (Fig. 6a). Room-temperature values of k_0 or H_c are not greatly different for the two samples but H_c decreases (and consequently k_i and k_0 increase) more rapidly with heating for the 110 μm grains. Thus, different sources of wall pinning, for example, a different mix of magnetocrystalline (rapid thermal decrease) and magnetoelastic (slower thermal decrease) anisotropies, can materially affect the presence and size of a Hopkinson peak.

The agreement between measured and predicted $k_0(T)$ is wellnigh perfect for the 14 μm magnetite sample (Fig. 6b). The dip, inflection and recovery of the $H_c(T)$ data at intermediate T (Fig. 4a) leads to a satisfying explanation of the hump in the $k_0(T)$ heating curve (red) near 250 °C. The much less noticeable hump in the cooling curve (blue) is also compatible with $H_c(T)$ data. The interpretation that initial internal strains due to crushing annealed out in heating seems reasonable. Even the ≈7 per cent increase in susceptibility after heating and cooling is accounted for. On the other

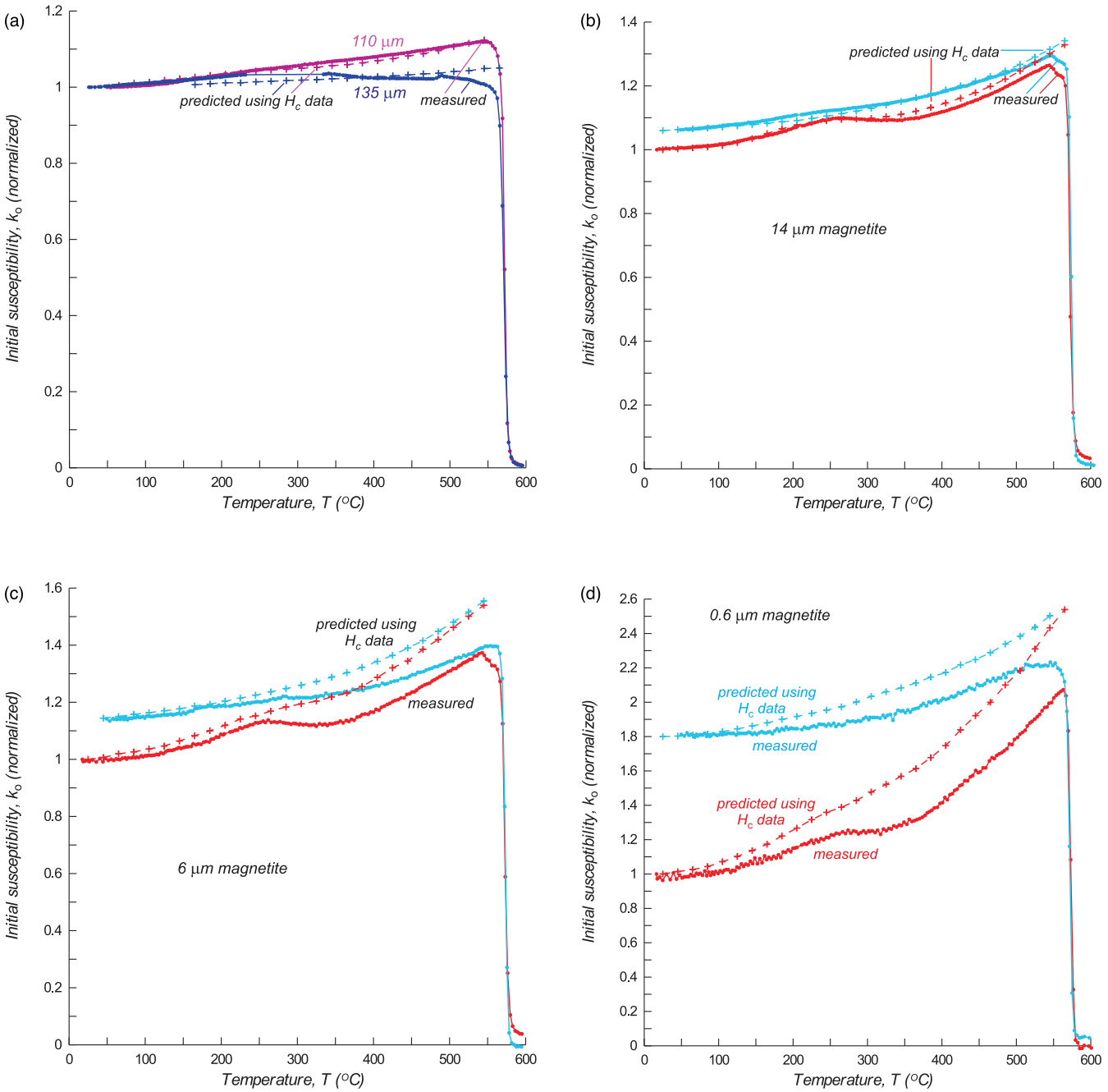

Figure 6. Comparison between measured $k_0 - T$ curves and predicted values (crosses) obtained by transforming measured H_c–T data (e.g. Fig. 4), first to $k_i - T$ and then to $k_0 - T$ pseudo-data (procedure described in the text). (a) The 110 μm magnetite cooling curve is well predicted, the 135 μm heating curve less so. (b) The 14 μm magnetite curves (red, heating; blue, cooling; both normalized to initial k_0 value at the beginning of the heating-cooling run) are well predicted, including the small hump around 250 °C, except for the details of the Hopkinson peak above 550 °C. (c), (d) The predicted curves rise progressively higher above the measured data as grain size decreases (6 and 0.6 μm samples illustrated), particularly for $T > 250$ °C, although the ratio between initial and final k_0 values at 20 °C continues to be accurately predicted. The disagreement could be due to a change in the shapes of wall energy barriers as T increases or to a previously unrecognized grain-size dependence of the empirical constant relating H_c and k_0 (see discussion in text).

hand, the ultimate height of the Hopkinson peak just below T_C is overestimated and the fine structure above 550 °C is not explained.

In smaller size fractions, the inflections in $H_c(T)$ data are less pronounced (Figs 4b and c) and only hint at the marked humps and inflections in the $k_0(T)$ curves (Figs 6c and d). The fit is reasonably good below ≈250 °C for the 6 μm sample (and also for the 3 and 1 μm samples) but not for the 0.6-μm magnetite. The ultimate Hopkinson peaks are overestimated by 10–30 per cent. It would seem that the shapes of energy wells have changed at high temperatures, that is, that the ratio between energy gradients low down and higher up in each well is different than before, so that k_i H_c no longer equals 45 kA m^{-1}. Another possibility is that the measured values of H_c are reduced by thermal fluctuations at the higher temperatures. This is conceivable if only small segments of walls are thermally activated but it is not a significant effect for entire walls.

The increasing misfit between prediction and measurement as grain size decreases (Figs 6b–d; grain sizes of 14, 6 and 0.6 μm, respectively) may reflect a real size variation in k_i H_c. Although no significant variation was seen in this size range in the data set used by Stacey & Banerjee (1974), Hodych (1986) reported a variation of about a factor 2 in the value of k_i H_c for 8 rocks with coercive forces ranging from ≈1 to ≈15 mT. Actual magnetite grain sizes in these rocks are not known but the H_c range matches that of the 3–135-μm magnetites in the present study (Table 1). Hodych's larger (less coercive) and smaller (more coercive) magnetites had k_i H_c values around 30 and 60 kA m^{-1}, respectively, with an average of 42 kA m^{-1} over the eight rocks (Hodych 1986, table II). A progressive increase in k_i H_c values for the smaller magnetites in the present study would have the effect of decreasing the predicted Hopkinson peaks to levels close to those observed.

7 CONCLUSION

PSD behaviour extends beyond TRM to the short-term induced magnetization of magnetite. Initial weak-field susceptibility k_0 of sized magnetite grains with mean dimensions of 0.6, 1, 3, 6, 9 and 14 μm and of rocks containing magnetite inclusions in silicates increases with rising temperature and reaches a Hopkinson peak just below the Curie point T_C. For 1-μm magnetites, the peak is 1.5 times k_0 at room temperature and even 14 μm grains have a peak of 1.25. Because domain walls move readily in response to the self-demagnetizing field created by any induced moment, MD grains are expected to have practically *T*-independent susceptibility but this is observed only for grains much larger than 14 μm, for example, 110 and 135 μm.

Hopkinson peak heights increase in a regular progression as grain size *d* decreases. Between 1 and 14 μm, $(k_0)_{max}/(k_0)_{20}$ values from both heating and cooling curves decrease linearly with log *d*. Limiting values of $(k_0)_{max}/(k_0)_{20} \approx 1$ for 110 and 135 μm grains fit on the extension of this trend. However, published values of $(k_0)_{max}/(k_0)_{20}$ for four submicron magnetites (King & Ranganai 2001) only fit the present trend in the case of the 0.1 μm sample. Peak heights of their 0.2, 0.5 and 1 μm size fractions are lower than the values reported here for 1–14 μm size fractions. Further measurements are needed to validate Hopkinson peaks as a granulometry technique.

Measurements of coercive force H_c as a function of temperature for the same sized magnetites used in the present susceptibility study shed light on the origin of the Hopkinson peaks. H_c is determined by maximum wall-energy gradient while intrinsic susceptibility k_i (response of walls to the net internal field) is inversely related to gradients near wall-energy minima. $H_c(T)$ data were transformed first to corresponding values of k_i and then through $k_0(T) = k_i(T)\,[1 + N\,k_i(T)]^{-1}$ to synthetic $k_0(T)$ data. Comparison of the measured and predicted $k_0(T)$ curves revealed that initial stress introduced in sample preparation and evident in the $H_c(T)$ data annealed out with heating, producing a noticeable hump in $k_0(T)$ curves at intermediate temperatures. Most importantly the overall shapes of $k_0(T)$ curves in both heating and cooling were reasonably well predicted, confirming the common dependence of susceptibility and coercive force on wall pinning.

Two rocks containing a bimodal mixture of coarse-grained magnetite and ultrafine magnetite inclusions in plagioclase exhibited Hopkinson peaks characteristic of both types of magnetite. For the Michael Gabbro, the Hopkinson peak height was 1.35. If oceanic layer-3 gabbros in situ at 500–600 °C temperatures have similar susceptibility enhancements, their contribution to magnetic anomalies may have been underestimated.

ACKNOWLEDGEMENTS

Helpful reviews and comments were provided by Jessica Till, Adrian Muxworthy and Eduard Petrovsky. Measurements were made at the Institute for Rock Magnetism, which is operated with support from the National Science Foundation, Earth Sciences Division and the University of Minnesota. Thanks to Mike Jackson and Peat Søleid for help with the instruments and operating programs. This research was supported by the Natural Sciences and Engineering Research Council of Canada.

REFERENCES

Arkani-Hamed, J., 1989. Thermoviscous remanent magnetization of oceanic lithosphere inferred from its thermal evolution, *J. geophys. Res.,* **94,** 17 421–17 436.

Clark, D.A. & Schmidt, P.W., 1982. Theoretical analysis of thermomagnetic properties, low-temperature hysteresis and domain structure of titanomagnetites, *Phys. Earth planet. Inter.,* **30,** 300–316.

Dubuisson, G., Pozzi, J-P. & Galdeano, A., 1991. Aimantation à haute température de roches profondes du forage continental du Couy (Bassin de Paris): discussion d'une contribution aux anomalies magnétiques, *C. R. Acad. Sci. Paris,* **312**(II), 385–392.

Dunlop, D.J., 1974. Thermal enhancement of magnetic susceptibility, *J. Geophys.,* **40,** 439–451.

Dunlop, D.J., 2002a. Theory and application of the Day plot (M_{rs}/M_s versus H_{cr}/H_c), 1. Theoretical curves and tests using titanomagnetite data, *J. geophys. Res.,* **107**(B3), 2056, doi:10.1029/2001JB000486.

Dunlop, D.J., 2002b. Theory and application of the Day plot (M_{rs}/M_s versus H_{cr}/H_c), 2. Application to data for rocks, *J. geophys. Res.,* **107**(B3), 2057, doi:10.1029/2001JB000487.

Dunlop, D.J., 2010. Magnetic properties of rocks of the Kapuskasing Uplift (Ontario, Canada) and origin of long-wavelength magnetic anomalies, *Geophys. J. Int.,* **183,** 645–658.

Dunlop, D.J., 2012. Magnetic recording in rocks, *Phys. Today,* **65**(6), 31–37.

Dunlop, D.J. & Özdemir, Ö., 1997. *Rock Magnetism: Fundamentals and Frontiers*: *Cambridge Studies in Magnetism*, Vol. 3, 573 pp, Cambridge Univ. Press.

Dunlop, D.J. & Özdemir, Ö., 2007. Magnetizations in rocks and minerals, in *Treatise on Geophysics,* **Vol. 5** Geomagnetism, pp. 278–336, ed. Schubert, G., Elsevier.

Dunlop, D.J., Zhang, B. & Özdemir, Ö., 2005. Linear and non-linear Thellier paleointensity behavior of natural minerals, *J. geophys. Res.,* **110,** B01103, doi:10.1029/2004JB003095.

Ferré, E.C., Geissman, J.W. & Zechmeister, M.S., 2012a. Magnetic properties of fault pseudotachylytes in granites, *J. geophys. Res.,* **117,** B01106, doi:10.1029/2011JB008762.

Ferré, E.C., Michelsen, K., Ernst, W.G., Boyd, J.D. & Canon-Tapia, E., 2012b. Vertical zonation of the Barcroft granodiorite, White Mountains, California: implications for magmatic processes, *Am. Miner.,* **97,** 1049–1059.

Halgedahl, S.L. & Fuller, M., 1983. The dependence of magnetic domain structure upon magnetization state with emphasis upon nucleation as a mechanism for pseudo-single-domain behavior, *J. geophys. Res.,* **88,** 6505–6522.

Harrison, R.J., Dunin-Borkowski, R.E. & Putnis, A., 2002. Direct imaging of nanoscale magnetic interactions in minerals, *Proc. Nat. Acad. Sci. USA,* **99,** 16 556–16 561.

Hodych, J.P., 1986. Determination of self-demagnetizing factor *N* for multidomain magnetite grains in rock, *Phys. Earth planet. Inter.,* **41,** 283–291.

Hopkinson, J., 1889. Magnetic and other physical properties of iron at a high temperature, *Phil. Trans. R. Soc. Lond,* **A. 180,** 443–465.

King, J.G. & Ranganai, R.T., 2001. Determination of magnetite grain-size using the Hopkinson effect – examples from Botswana rocks, *Botswana J. Earth Sci.,* **5,** 35–38.

King, J.G. & Williams, W., 2000. Low-temperature magnetic properties of magnetite, *J. geophys. Res.,* **105,** 16 427–16 436.

King, J.G., Williams, W., Wilkinson, C.D.W., McVitie, S. & Chapman, J.N., 1996. Magnetic properties of magnetite arrays produced by the method of electron beam lithography, *Geophys. Res. Lett.,* **23,** 2847–2850.

Kiss, J., Szarka, L. & Prácser, E., 2005. Second-order magnetic phase transition in the Earth, *Geophys. Res. Lett.,* **32,** L24310, doi:10.1029/2005GL024199.

Kiss, J., Prácser, E. & Szarka, L., 2008. Consequences of magnetic phase transition in the Earth's crust, in *Proc. Conf. Magn. Geomag. Biomag. MGB–2008,* 7–8 Nov. 2008, Sezana, Slovenia, pp. 7–10.

Kontny, A. & de Wall, H., 2000. The use of low and high k(T) curves for the characterization of magneto-mineralogical changes during metamorphism, *Phys. Chem. Earth,* **25,** 421–429.

Özdemir, Ö., Xu, S. & Dunlop, D.J., 1995. Closure domains in magnetite, *J. geophys. Res.,* **100,** 2193–2209.

Pozzi, J-P. & Dubuisson, G., 1992. High-temperature viscous magnetization of oceanic deep crustal- and mantle-rocks as a partial source for Magsat magnetic anomalies, *Geophys. Res. Lett.,* **19,** 21–24.

Roberts, A.P., Pike, C.P. & Verosub, K.L., 2000. First-order reversal curve diagrams: a new tool for characterizing the magnetic properties of natural samples, *J. geophys. Res.,* **105,** 28 461–28 475.

Shive, P.N. & Fountain, D.M., 1988. Magnetic mineralogy in an Archean crustal section: implications for crustal magnetization, *J. geophys. Res.,* **93,** 12 177–12 186.

Stacey, F.D. & Banerjee, S.K., 1974. *The Physical Principles of Rock Magnetism,* 195 pp, Elsevier.

Szarka, L., Franke, A., Prácser, E. & Kiss, J., 2007. Hypothetical mid-crustal models of second-order magnetic phase transition (extended abstract), in *4th International Symposium on 3-Dim. Electromagnetics*, 27–30 Sept. 2007, Freiberg, Germany, 4 pp.

Szarka, L., Kiss, J., Prácser, E. & Ádám, A., 2010. The magnetic phase transition and geophysical crustal anomalies, *Chinese J. Geophys.,* **53**(3), 612–621.

Williams, M.C., Shive, P.N., Fountain, D.M. & Frost, B.R., 1985. Magnetic properties of exposed deep crustal rocks from the Superior Province of Manitoba, *Earth planet. Sci. Lett.,* **76,** 176–184.